Bulletin of Electrical Engineering and Informatics
Vol. 13, No. 2, April 2024, pp. 702~712
ISSN: 2302-9285, DOI: 10.11591/eei.v13i2.5870

Solar power forecasting model as a renewable generation source on virtual power plants

Suwarno[1], Doni Pinayungan[1,2]
[1]Electrical Engineering Study Program, Postgraduate Program, Universitas Muhammadiyah Sumatera Utara, Medan, Indonesia
[2]Faculty of Engineering, Institut Teknologi dan Sain Padang Lawas, Padang Lawas Utara, Indonesia

Article Info

Article history:

Received Jan 27, 2023
Revised Jul 28, 2023
Accepted Aug 31, 2023

Keywords:

Mean absolute error
Root mean square error
Photovoltaic
Solar power management
Sun forecast
Virtual power plants

ABSTRACT

This paper describes modeling solar power generation as a renewable energy generator by simulating the analytical approach mean absolute error and root mean square error (MAE and RMSE). This research estimates the error referring to long short-term memory (LSTM) network learning. Related to this, the Indonesian government is currently actively developing solar power plants without ignoring the surrounding environment. The integration of solar power sources without accurate power prediction can hinder the work of the grid and the use of new and renewable generation sources. To overcome this, virtual power plant modeling can be a solution to minimize prediction errors. This study proposes a method for on-site virtual solar power plant efficiency with a research approach using two models, namely RMSE and MAE to account for prediction uncertainty from additional information on power plants using virtual solar power plants. A prediction strategy verified against the output power of photovoltaic (PV) modules and a set based on data from meteorological stations used to simulate the virtual power plants (VPP) model. This forecast prediction refers to the LSTM network and provides forecast errors with other learning methods, where the approach simulated with 12.36% and 11.85% accuracy for MAE and RMSE, respectively.

Corresponding Author:

Suwarno
Electrical Engineering Study Program, Postgraduate Program, Universitas Muhammadiyah Sumatera Utara
Denai Road, No. 217, Medan, Indonesia
Email: suwarno@umsu.ac.id

1. INTRODUCTION

The involvement of energy use continues to increase resulting in the availability and stability of world energy commodity prices, but also opportunities for cooperation as well as competition between countries in the Asia Pacific region. Indonesia is currently planning to continue developing renewable energy with a policy of around 23% of its energy being supplied by modern renewable energy by 2025, with at least 31% coming from modern renewable energy sources by 2050. According to the international energy agency (IEA), energy demand continues to increase by around 30% by 2015-2040 [1]. PT PLN has discontinued several steam power plants until 2056, with initial participation in 2030 and concentrating on renewable energy [2].

Solar energy is an effective form of solar energy and a renewable energy solution that can reduce the greenhouse effect and global warming [3]. Indonesia has a renewable energy potential of 4.80 kWh/m^2/day and only uses 10 MWp in 2024 [4], whereas Indonesia has relatively large solar energy of around 0.87 GW in 2025 [5]. In addition, Indonesia also produces electricity from solar energy with a potential of around 640,000 TWh per year, thus enabling the achievement of energy mix targets that can reduce greenhouse gas emissions through the development of renewable energy [6]. Market demand for solar energy has been driven by government incentives and tax breaks for installing solar panels and increasing environmental pollution [7]. The need for renewable energy in the global market continues to increase by around 25.9% until 2030 [8]. Several factors are driving the spread of solar energy, including the decline in the price of solar panels, and environmental, political, social, and cultural issues. Based on research from Sovacool *et al.* [9] that, global installed capacity is affected by identified constraints including the pace of achieving solar dominance, lack of investment for efficiency, and regulations governing the distribution of solar power. Coordination of photovoltaic (PV) installations with virtual power plants (VPP) power generation models for global production prediction provides accurate values integrated into the network [10].

Strategy and power prediction at PV and prediction interval chosen for PV facilities in the VPP model can be replicated for real PV and can improve high accuracy with two models mean absolute error and root mean square error (MAE and RMSE) with values of 12.37% and 11.84% respectively [11], [12]. The limitations of technology in the past have an impact on the current electricity network, so it is necessary to fundamentally restructure fossil energy to serve the energy needs of renewable energy in the future [13]. Integral part and participation of energy resources distributed and decentralized small-scale power generation units with traditional power generation passively limited to the existing distribution network [14]. One possible solution is to combine renewable energy sources (RES) by coming up with the idea of a VPP, which is described as a collection of various DERs that function as one unit [15]. The general description of the VPP model has been discussed in real-life research [16]–[18]. Power system design with a high proportion of RES is an important part of the renewable energy system change [19], [20]. This methodology is based on QRF modeling to obtain optimal supply from automatic frequency recovery reserves provided by renewable power aggregation [21].

Switching to new and renewable energy can help reduce greenhouse gas emissions by limiting the impact of extreme weather and climate while supplying reliable, timely, and cost-effective energy. PV breakthroughs can be attributed to the increased integration of PV systems into VPPs, which makes this energy sales model difficult to implement due to regulatory constraints [22]. The VPP model is the ultimate solution offering for reducing the carbon footprint of conventional power grids and the integration of PV and wind [23]. This VPP addresses sudden climate change resulting from PV output as well as the management of other energy requirements under the same VPP [24]. Major divisions of uncertainty need to be managed by the VPP [25]. A common solution for managing PV uncertainty is to invest in energy-storage capabilities in batteries [26]. However, the VPP model is expected to have real-time operational capacity to match the pre-designed plans based on other PV forecasts [27]. An alignment is performed to get a match from the previous market quote to execute a second VPP order on a real market trade [28]. The VPP model deals with distributed data collection and management of distributed energy sources to meet certain optimizations [22]. VPP discovery and modeling involve complex information and computer techniques related to modeling and energy flows [24]. The concept and technology used for VPP are shown in Figure 1.

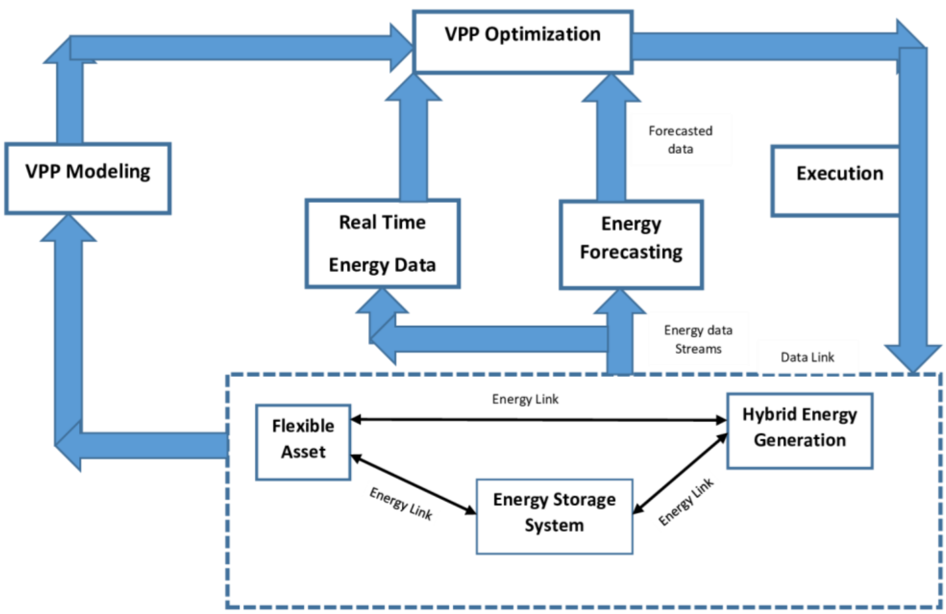

Figure 1. Concept of energy and technology used for VPP

Energy predictions together with load demand and energy financing, at different times and resolutions, are entered into the equation model. VPP model prediction methods can be differentiated according to different factors, for example, parameters to be forecast (radiation), time and resolution constraints, waiting times, model predictions, and statistical properties of forecasting [29]. The model directly predicts PV through PV datasets and past climate conditions. Indirect forecasting is the prediction of solar radiation and solar energy that can be calculated using a PV performance model [30]. Some consideration of intervals for predictions and expected uncertainties can provide additional information in making judgments and can provide a reasonable number of values and assigned probabilities of those values [31]. To solve this problem, the researcher presents an approach to predict PV power by using program tools for the locations studied.

The contribution of this proposed paper is modeling solar power as a virtual generator and prediction using the Rayleigh model with the main contributions being; i) the PV prediction model obtained at VPP to minimize forecasting errors by modeling a two-parameter function; ii) the prediction interval time for modeling the prediction uncertainty is a function that depends on hold time and launch time with cloud cover factor (CCF); and iii) data input strategy for this prediction comes from data sources that have open access and are free in cost savings in the VPP model.

2. METHOD

2.1. Proposed method

The strategy of the proposed daily power forecasting framework is shown in Figure 2 to predict the proposed daily power, consisting of data input and power prediction preprocessing, and the VPP model. Several steps for input data preprocessing as used in training and prediction models. The expected output of the prediction algorithm is the energy management system (EMS) input of the observed VPP. Numerical weather prediction (NWP) module for irradiation forecasting design and training to estimate power given input data from NWP model to generate VPP model after correction by EMS. This process continues until the expected solar power plant is produced.

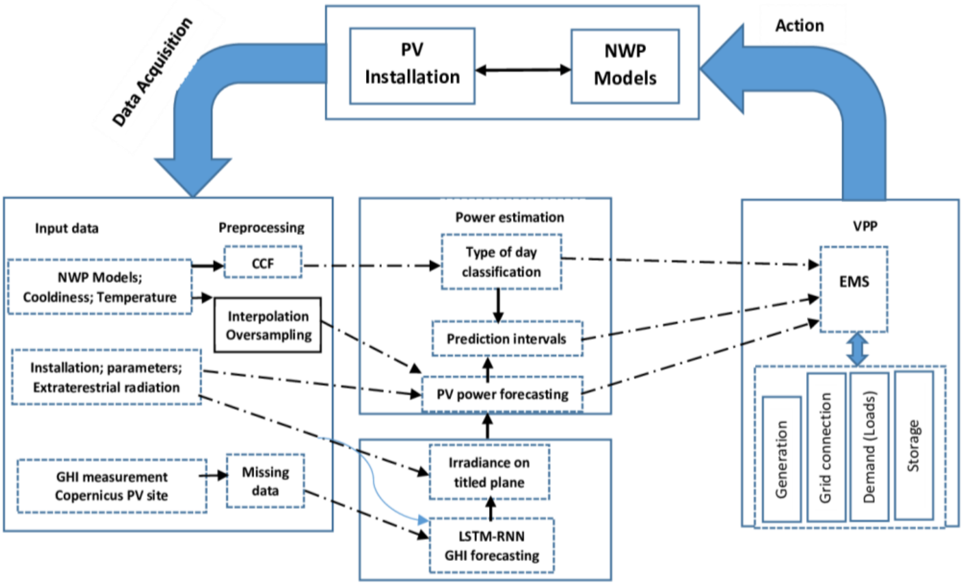

Figure 2. Proposed forecasting framework

2.2. Enter data

The input data consists of several classifications that are tailored to the source and information required. The first input data consists of turbidity and temperature derived from prediction maps with scales obtained from the meteorology, climatology, and geophysics agency (MCGA). The radiation turbidity prediction data is intended to determine the CCF, which can indicate the cloud area on the shadow NWP-based turbidity map at the PV installation. This parameter determines the type: sunny, cloudy, and overcast. It is expected to obtain a set of data that can be assigned to different groups in terms of making prediction intervals. Where temperature data is used to estimate the temperature of solar panel cells during prediction [31]. Climate maps based on NWP are particularly interesting because of some useful weather changes that may not be available at solar installations. Deviations in cell temperature forecasts were assessed using data obtained from MCGA. A prediction model with MAE was implemented for temperature corresponding to the NWP map of 2.13°C obtaining a power of 46.96 W/m^2, for measurements throughout the year. The prediction modeling of the dataset for training purposes consists of the sun position, which is used in the CCF calculation to determine the daily data, while the space radiation is used as a prediction, and the radiation on the inclined plane of the PV module location.

2.3. Data pre-processing

To predict the PV power consisting of cell temperature and irradiance on the inclined plane, it is necessary to perform quadratic interpolation to predict the NWP. The temperature changes around the study can be assumed for the NWP map as proposed by [32]. The exact substantiation with the one-year approximation model is shown in Table 1, which illustrates that the ambient temperature is obtained from the predicted value measured from the MCGC station for PV module modeling. This parameter allows the daily radiation to influence the identification of a specific period to change the PV module in the period of the presence of clouds to change the PV generation in the region by preventing the solar radiation which gives an exact picture of the calculation of the detected parameters [33].

Table 1. Performance model matrix

Metrics	Scale (W/m^2)	Percentage (%)
Absolute	$MAE = \frac{1}{T}\sum_{t=1}^{T}\left\|Y_t - \hat{Y}_t\right\|$	$rMAE = \frac{\frac{1}{T}\sum_{t=1}^{T}\left\|Y_t = \hat{Y}_t\right\|}{\frac{1}{T}\sum_{t=1}^{T}Y_t} x100\%$
Square	$RMSE = \sqrt{\frac{1}{T}\sum_{t=1}^{T}\left(Y_t - \hat{Y}\right)}^2$	$rRMSE = \frac{\sqrt{\frac{1}{T}\sum_{t=1}^{T}\left(Y_t - \hat{Y}\right)^2}}{\frac{1}{T}\sum_{t=1}^{T}Y_t} x100\%$

2.4. Irradiance modeling and prediction

Prediction of solar irradiation based on Rayleigh modeling with the aim of i) obtaining the average power of the PV model for 30 minutes each day on PV modules and ii) looking at possible uncertainties in the forecast results [34]. The data information in Table 1 shows the main inputs for the EMS on the VPP module. The modeling and prediction results are shown in Figure 3. To minimize the error of the training process by calculating the RMSE and considering the mismatch of the corresponding system, but also considering the computation time. Prediction of effective solar radiation on the inclined plane of the PV module. The first is to calculate the effective irradiation using data from two irradiating elements on a plane, either direct or diffuse. In this case, the albedo is zero and is estimated as a function of the clarity index (*kth*) to account for the mass transfer fraction *(k)dh* [35]. Based on this information, the conversion to an inclined plane is approximated by diffuse radiation and albedo [36]:

$$\text{albedo} = r_0 \text{ghm}_0(1 - \cos\beta)/2 \tag{1}$$

Where r_o is the albedo coefficient, with a value of 0.2 ghm$_0$ as the global horizontal irradiance (GHI) and β as the panel tilt angle. The effective radiation is determined by considering the angular loss [37] and spectral [38] with the p-Si module and medium dust level at DT 0.97 for installation. Model for converting PV power from its effective solar radiation [39].

$$P_{\text{DC}} = \text{SF}\eta_{\text{DC}}P_{\text{peak}}\frac{G_{\text{panel}}}{G_{\text{STC}}}\left(1 + \delta P_m(T_{\text{cell}} - T_{\text{cell,STC}})\right) \tag{2}$$

Where P_{DC} is the PV estimate, *SF* serves as a representation of the shadow loss caused by the environment, for this particular case, η_{DC}=0.928 including cable losses, with module tolerance and mismatch losses; P_{peak}=2.98 kW as the peak power of the installation, G_{panel} serves as the useful solar radiation of the calculated panel, G_{STC} is 1 kW/m^2 which is the solar radiation under standardized testing conditions with (STC), δPm is 0.4%/°C which is the temperature change of the PV panel installation, T_{cell} as a function of cell temperature, and $T_{cell,\ STC}$ is the cell temperature under STC. The determination of cell temperature is expressed by (3), ignoring wind speed, which is a complex effect that is insignificant to the model and does not affect the panel facility uniformly [40]:

$$T_{\text{Cell}} = \frac{T_{\text{Cell,NOCT}} - T_{\text{amb,NOCT}}}{G_{\text{NOCT}}} G_{\text{panel}} + T_{\text{amb}} \quad (3)$$

Where $T_{cell,\ NOCT}$=45ºC represents the cell temperature as a function of normal operating cell temperature (NOCT); $T_{amb,\ NOCT}$=20ºC is the ambient temperature under NOCT conditions; G_{NOCT} is 800 W/m^2 which is the solar radiation under NOCT conditions; and T_{amb} is the ambient temperature resulting from NWP predictions.

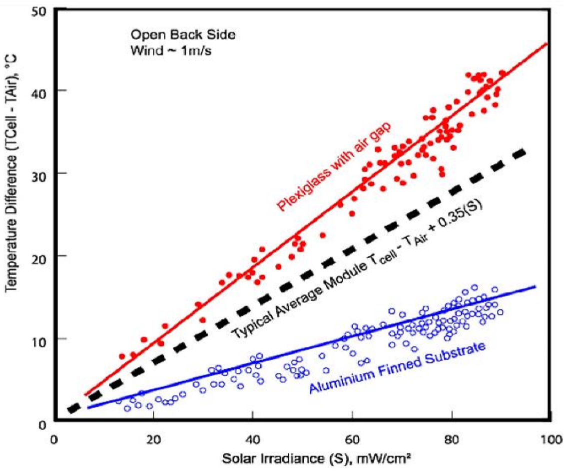

Figure 3. Illustration of solar radiation at NOCT

After all the datasets related to PV prediction, it can calculate the prediction interval to predict the new one. A prediction interval is a prediction interval with a random variable to judge in the future whose magnitude is unknown [41]. In this paper, tabulated prediction intervals are used based on research that has been done considering the Laplacian distribution model for errors as a function of lead time, launch time, and day type [42].

Temperature changes between the module and the air caused by solar radiation can result in heat transfer losses and faster heat transfer that occurs in solar insulation damage for a given wind speed with thermal resistance and heat transfer coefficients that do not vary much with temperature changes. In Figure 3, it can be seen that the change in NOCT for some PV modules in the best case, worst case, and average in the best case resembles aluminum fins on the back of the module for cooling which lowers the thermal resistance and increases the surface area for heat transfer in other media. Figure 4 shows the time interval for 90% daily which has provided valuable additional information from this prediction. PV generation is highly dependent on weather conditions and seasonal changes. This can affect the ability of the prediction algorithm to calculate a precise prediction and can provide some level of uncertainty that should be evaluated. Prediction levels are used to express the level of uncertainty at the point of forecasting which adds to a given confidence level.

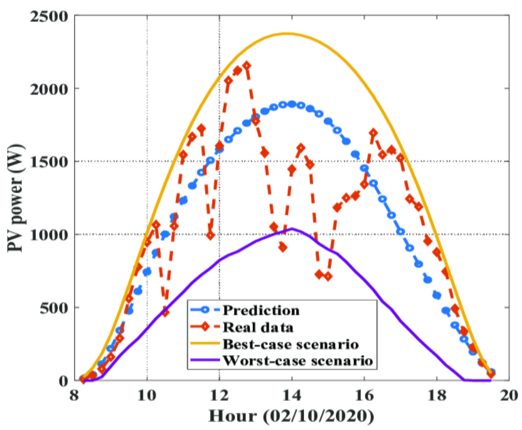

Figure 4. Interval prediction for PV

3. RESULTS AND DISCUSSION

The research results for this study, obtained from the proposed daily forecasting strategy for VPP generation modules can be differentiated in several ways, namely: i) PV power estimation from the forecasting output; ii) prediction interval quantitative assessment; and iii) VPP module schedule. First, the research results are validated against PV module installations acting as VPP nodes. Secondly, a strategy is developed for a replicated VPP model using data-driven meteorological stations. The proposed model is evaluated by its effectiveness and compared to its performance to determine its accuracy compared to methods proposed in other literature.

3.1. Predictions for virtual power plants nodes

Forecasting for real VPP nodes is performed using irradiance measurements taken at existing PV facilities at MCGA. GHI forecasting can provide a launch and wait function with a specified time and parameters in the future to calculate the prediction interval. The associated error rating will depend on the following two model metrics: i) the dependence of the metrics on the *MAE* and *RMSE* scales and ii) the percentage error of the *rMAE* and *rRMSE* metrics. The metrics give an idea of the absolute value of the average forecasting information, but the squared value is more sensitive to data deviating from the average data and it is the analysis of both that makes it possible to study the overall prediction results.

A magnitude of the error ratio value that also gives an understanding of what is being done to the error is a fair comparison for dependability, but as it approaches zero, a scale-dependent metric is the preferred choice. Table 1 is a performance matrix for the value of Y, which is the measured data from time t, $\hat{Y}_t$ is the forecast value for time t, and T is the length of consecutive times that can be used to provide a value for the accuracy of the algorithm.

The values Y_{tt}, and Y_{tot} are predictions of Y_t at t_0 and t_0 is the predetermined start time for each day equivalent to sunrise. With the error assessment of the two parameters, it is necessary to determine the amount of lead time and launch time. The exact waiting time at (t'-t) gives the difference between the specified waiting time and the predicted launch time. The launch time is indicated by (t'-t_o) and is the difference between the current time and sunrise. The launch time and waiting time for a specific day prediction are described in Figure 5, where the launch time is set and the waiting time is used as a parameter, The prediction vector is obtained when the two parameters are set to specific values.

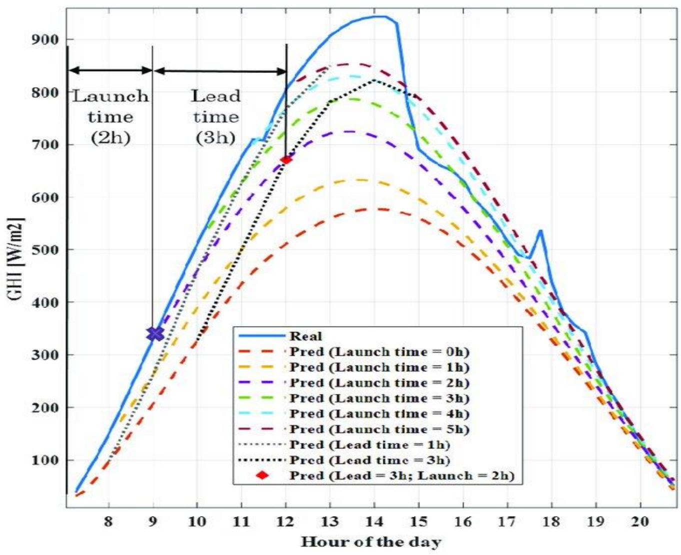

Figure 5. Measurement and prediction results

Figure 5 illustrates the errors in lead time and launch time leading to the following conclusions. First, for the scaling error, a high error rate is observed for short launch times under a moderate timeout. It is expected that the scaling error will be mostly under the former setting with high solar radiation, but as the launch time increases, this error is significantly reduced. Secondly, the lower the solar radiation, the smaller the error scale, and for the error percentage it will be the opposite; when the launch time is small (smaller than 1 hour), the high error percentage will be independent of the time limit [43]. Finally, the forecasting interval derived from the MAE, possibly a distribution given by dividing the prediction as a function of lead time, launch time, and type of day would be particularly useful at the high level of accuracy required for the prediction. The predictions obtained with the forecasting error in this study are much smaller at short lead times. The comparison strategy described in this paper regarding estimation can be concluded, that small lead times will result in better estimates compared to traditional methods [44].

3.2. Photovoltaic prediction from global horizontal irradiance forecast

To estimate the PV model from the GHI prediction there are several steps, namely i) instantaneous time prediction; ii) surveying the location from altitude, latitude, and longitude; iii) installation performance covered in the orientation and inclination of the panels, the PV model identifying the parameters available in the data sheet and the losses associated with each part of the installation; and iv) from the NWP map on the ambient temperature. For the above purposes, it is necessary to perform an analysis technique that allows us to quantify the errors made in solving the problem. The results of two different approaches consist of: first, making a comparison between the actual PV measurements at the site and the estimated PV values from the GHI measurements. Second, the PV module is predicted from the GHI estimated values and evaluates the errors associated with all these processes. The main GHI looks for the error value obtained to maintain the same performance as obtained in the previous section by using the error to build the prediction interval. Figure 4 is a comparison between the measured value of the PV module at the site and the estimated PV obtained from the GHI measurement at the site. Choose from three types of days namely; cloudy days, cloudy days, and sunny days [45]. The x-axis is the solar time function and the y-axis is the GHI to be sought. For the experimental setup at the studied site which has buildings near the PV panels that provide partial shading until sunset. Figure 4 is a comparison between the measured value of the PV module at the site and the estimated PV obtained from the GHI measurement at the site. Choose from three types of days namely; cloudy days, cloudy days, and sunny days. The x-axis is the solar time function and the y-axis is the GHI to be sought. For the experimental setup at the site under study which has buildings near the PV panels that provide partial shade until sunset. Figure 5 is a comparison between the measured value of the PV module at the site and the estimated PV obtained from the GHI measurement at the site. Choose from three types of days namely; cloudy days, cloudy days, and sunny days. The x-axis is the solar time function and the y-axis is the GHI to be sought. For the experiment setup at the site under study which has buildings near the PV panels that provide partial shade until sunset.

The modeling of this condition is expressed in (2), assuming that the change is linear with time as shown in Figure 5 with SF 0.95 at 16:36, decreasing to SF 0.4 at sunset, and also varying depending on the season of the year [46] obtained an rMAE value of 2.55% for sunny days, a rMAE=3.05% for partly cloudy days, and an increased rMAE value of 4.04% for cloudy days. Observations based on the square error, where the rRMSE value is 3.44% on sunny days and the rRMSE is 3.89% on partly cloudy days, up to an rRMSE of 5.96% for cloudy days. The transition characteristics of the MPPT inverter control in the presence of passing clouds cause the inverter operational point to become unstable. This increases the daily error but does not cause problems in the forecasting process with a time difference of about 15 minutes which can reduce the negative effect. Figure 5 illustrates the estimation error resulting from the difference between measured and estimated PV modules as a function of lead time and launch time so it has a similar picture to the previous figure, with almost the same percentage error. It can be concluded that it is almost the same as that achieved in Figure 5 so it can be stated that: i) short launch times and moderate lead times result in high scaling, but decrease significantly with increasing launch time; ii) launch times of less than one hour result in high error rates that appear to be independent of lead time; and iii) high error rates at lead times above 7 hours.

3.3. Estimated photovoltaic power interval

Additional information for prediction intervals over a reasonable range of PV power generated at a given location and confidence level is selected by the user. Taking a prediction interval can increase the uncertainty in the point estimation and can avoid unexpected energy shortage or, conversely, energy overload, which is less important than the former because the inverter can change its operating point to produce the required energy, although wasting the required energy resources can be overused. In this paper, the prediction intervals are obtained based on the operations performed by [47]. The results depend on the accuracy of the estimation of the delay time and launch time. The factual results used aim to divide the forecast data set and create groups, assuming that a certain distribution is built on the MAE. This group division is determined when choosing the launch time and lead time where approximately 365 samples per batch are obtained in a full year. Figure 5 shows different error distributions for launch time values of 2, 4, and 6 hours, with lead time values of 1, 2, and 3 hours. In the assumed Laplacian distribution, this is similar to the work done by the CCF function. The prediction interval for each subset can be determined by the MAE assuming that it is for the Laplacian distribution [48]. A more detailed subdivision can be determined with the groups selected as a function of the CCF but must take into account the number of groups as presented earlier with insufficient samples from each group to create a proper error distribution [48].

Mitigate this weakness by reducing the number of CCF groups to three and using the type of day classification described above. The study size with CCF has an hourly decision with a value of zero when the sun is not obscured by clouds and one when the sun is completely covered by clouds. The k-nearest neighbor (k-NN) method is usually used to form clusters that allow the dataset to be divided simply and offer an independent solution for each object in the VPP. Assuming that for the Laplacian distribution, each new subset selected carries an error that needs to be measured. Coverage probability interval prediction [49] indicates the share of predicted values that fall within the selected interval and are close to the confidence level. The confidence level chosen in this study is 80%, although this number can be modified depending on the operational risk to be addressed by high-risk objects and thus the higher the usefulness of the tool.

3.4. Discussion

The technical development of VPP should be supported by current EMS technologies with PV modules expected to be a very important part. The energy generated by each VPP node referring to renewable sources allows for optimization of the expected benefits of energy exchange with the grid operator. It is difficult to predict PV modules when it is necessary to collect information from several nodes spread over a large area especially when the input data required to predict is expensive. This research proposes a way to achieve this goal by using a strategy based on LSTM-RNN by forecasting the GHI using a dataset of solar radiation values obtained from direct satellite data and then the solar energy utilized by PV installations [50], [51]. First of all, it provides results for the GHI estimation for installation based on hold time and launch time, which allows regions with lower errors and high confidence levels to be generated in the form of day-type-dependent prediction intervals. The GHI error is a function of the hold time and launch time, which shows low behavior when the launch time is lower than 1.5 hours, based on sunrise. To avoid this, the forecasting process can start 1.5 hours after sunrise. This proposed study can rely on a few days ahead prediction made to obtain solar radiation forecasts [52]. An assessment of the accuracy and rigor of the safety forecasts and the results were compared with the literature, with results similar to those obtained from deep learning algorithms and outperforming existing traditional techniques.

The difference between waiting time and launch time makes it possible to compare which one is better about the literature, but it is difficult to conclude if the study is done with only one value, where MAE is related to each other without considering waiting time and launch time with a value of 44.18 W/m^2 which has similarities with other studies. After the solar irradiance is estimated, the PV is then converted and calculated analytically with minimized errors, which are 2.55-4.04% for the rMAE value and 3.45-5.95% for the rRMSE. The shape of the error matrix shows similar results to those presented above, so it can be concluded that the generalized and performed MAE, in this case, is 137.22 W facilitated by 2.97 kWp PV [53]. The prediction interval is chosen once it is possible to obtain an estimate of the available PV power within an acceptable range of point estimate values. The method considers the Laplacian error distribution and distinguishes between waiting time, launch time, and day type, which are selected by using the instructions of the k-NN as a CCF function. The confidence level can be maintained by verifying the calculated PICP and a value of 80% is obtained. These results show that there is a clear difference between the PICP and the confidence level on cloudy days before sunset, but for predictions at these hours, it is not very important, so it can be concluded that the chosen prediction interval is very relevant.

The results show that the reduction of RMSE error is influenced by several important factors affecting accuracy and the strategy used [54]. PV generation systems are one of the easiest and most cost-effective renewable energy sources (RES) that can be utilized in households and it is possible to convert PV modules into customizable PLTS nodes [55]. Ultimately, indirect prediction predictions for PV system performance models are required to obtain solar power generation predictions. Strategies used to predict performance under irradiation and temperature conditions should be adopted [56]. At the specified operational location of PV panels, alternative methods can be obtained [57] and can improve accuracy, while other studies use a calculated whole-population model to simplify the process [58]. Finally, PV power estimates were made and prediction intervals were selected for PV module facilities. It can be concluded that the VPP environment and PV facilities at the weather station can be simulated with an accuracy of 12.36% against MAE and 11.85% against RMSE.

4. CONCLUSION

Based on the results of the discussion above, it is concluded that the forecasting model for solar power sources as a virtual solar generator uses statistical analysis and evaluation with MAE and RMSE. These two models are generally used to calculate the prediction error of a data series, with the advantages and disadvantages of each model, so that the modeling decision is determined by the type of data to be managed in the study. Power prediction research at PV generators and prediction intervals were chosen for

PV module facilities where the VPP model environment and PV facilities at weather stations could be simulated with an accuracy of 12.36% (0.1236) against MAE and 11.85% (0.1185) against RMSE. For forecasts derived from MAE, the distribution given by dividing the predictions is a function of lead time, launch time, and type of day which will be very useful at the high level of accuracy required for prediction. The predictions obtained with forecasting errors in this study are much smaller at short waiting times. The comparison strategy described in this paper regarding estimation, namely with a short waiting time, will produce better estimates compared to traditional methods which have similarities with other studies. The error matrix form shows results similar to those presented above, so the MAE method is more commonly used in research cases. Modeling assumes that the change is linear with time with SF decreasing at sunset, and also varies by the season of the year to get rMAE values, for sunny days, partly cloudy. Observations based on RMSE give results on sunny, partly cloudy, and cloudy days. Apart from MAE and RMSE, the main GHI is also calculated to find the error values obtained to maintain the same performance as obtained in the previous section by using errors to build prediction intervals. Which metric is best depends on the use case and research data set. However, RMSE is usually the preferred metric over MAE for measuring model performance. This is because developers often want to reduce the appearance of large outliers in their predictions and the MAE is considered too simple to understand the overall model performance.

ACKNOWLEDGEMENTS

The author would like to thank the leadership of the Universitas Muhammadiyah Sumatera Utara for supporting this research, especially the research laboratory that has been provided for this research. This research is independent and funded by the researchers themselves and thanks to all parties.

REFERENCES

[1] T. Ahmad and D. Zhang, "A critical review of comparative global historical energy consumption and future demand: The story told so far," *Energy Reports*, vol. 6, pp. 1973–1991, Nov. 2020, doi: 10.1016/j.egyr.2020.07.020.

[2] T. Jałowiec, H. Wojtaszek, and I. Miciuła, "Analysis of the Potential Management of the Low-Carbon Energy Transformation by 2050," *Energies*, vol. 15, no. 7, p. 2351, Mar. 2022, doi: 10.3390/en15072351.

[3] N. Belyakov, "Solar energy," in *Sustainable Power Generation*, Elsevier, 2019, pp. 417–438, doi: 10.1016/B978-0-12-817012-0.00031-1.

[4] N. A. Pambudi *et al.*, "Renewable Energy in Indonesia: Current Status, Potential, and Future Development," *Sustainability*, vol. 15, no. 3, p. 2342, Jan. 2023, doi: 10.3390/su15032342.

[5] H. Hardianto, "Utilization of Solar Power Plant in Indonesia: A Review," *International Journal of Environment, Engineering and Education*, vol. 1, no. 3, pp. 1–8, Dec. 2019, doi: 10.55151/ijeedu.v1i3.21.

[6] D. F. Silalahi, A. Blakers, M. Stocks, B. Lu, C. Cheng, and L. Hayes, "Indonesia's Vast Solar Energy Potential," *Energies*, vol. 14, no. 17, p. 5424, Aug. 2021, doi: 10.3390/en14175424.

[7] U. Kılıç and B. Kekezoğlu, "A review of solar photovoltaic incentives and Policy: Selected countries and Turkey," *Ain Shams Engineering Journal*, vol. 13, no. 5, p. 101669, Sep. 2022, doi: 10.1016/j.asej.2021.101669.

[8] T. Ranta, M. Laihanen, and A. Karhunen, "Development of the Bioenergy as a Part of Renewable Energy in the Nordic Countries: A Comparative Analysis," *Journal of Sustainable Bioenergy Systems*, vol. 10, no. 03, pp. 92–112, 2020, doi: 10.4236/jsbs.2020.103008.

[9] B. K. Sovacool, M. L. Barnacle, A. Smith, and M. C. Brisbois, "Towards improved solar energy justice: Exploring the complex inequities of household adoption of photovoltaic panels," *Energy Policy*, vol. 164, p. 112868, May 2022, doi: 10.1016/j.enpol.2022.112868.

[10] J. Liu, H. Hu, S. S. Yu, and H. Trinh, "Virtual Power Plant with Renewable Energy Sources and Energy Storage Systems for Sustainable Power Grid-Formation, Control Techniques and Demand Response," *Energies*, vol. 16, no. 9, p. 3705, Apr. 2023, doi: 10.3390/en16093705.

[11] G. Moreno, C. Santos, P. Martín, F. J. Rodríguez, R. Peña, and B. Vuksanovic, "Intra-Day Solar Power Forecasting Strategy for Managing Virtual Power Plants," *Sensors*, vol. 21, no. 16, p. 5648, Aug. 2021, doi: 10.3390/s21165648.

[12] Z. Ullah, N. H. Mirjat, and M. Baseer, "Optimisation and Management of Virtual Power Plants Energy Mix Trading Model," *International Journal of Renewable Energy Development*, vol. 11, no. 1, pp. 83–94, Feb. 2022, doi: 10.14710/ijred.2022.39295.

[13] S. K. Rangu, P. R. Lolla, K. R. Dhenuvakonda, and A. R. Singh, "Recent trends in power management strategies for optimal operation of distributed energy resources in microgrids: A comprehensive review," *International Journal of Energy Research*, vol. 44, no. 13, pp. 9889–9911, Oct. 2020, doi: 10.1002/er.5649.

[14] Z. Ullah and N. H. Mirjat, "Modelling and analysis of virtual power plants interactive operational characteristics in distribution systems," *Energy Conversion and Economics*, vol. 3, no. 1, pp. 11–19, Feb. 2022, doi: 10.1049/enc2.12033.

[15] E. Sarker *et al.*, "Progress on the demand side management in smart grid and optimization approaches," *International Journal of Energy Research*, vol. 45, no. 1, pp. 36–64, Jan. 2021, doi: 10.1002/er.5631.

[16] M. M. Roozbehani, E. Heydarian-Forushani, S. Hasanzadeh, and S. B. Elghali, "Virtual Power Plant Operational Strategies: Models, Markets, Optimization, Challenges, and Opportunities," *Sustainability*, vol. 14, no. 19, p. 12486, Sep. 2022, doi: 10.3390/su141912486.

[17] Z. Ullah, Arshad, H. Hassanin, J. Cugley, and M. Al Alawi, "Planning, Operation, and Design of Market-Based Virtual Power Plant Considering Uncertainty," *Energies*, vol. 15, no. 19, p. 7290, Oct. 2022, doi: 10.3390/en15197290.

[18] G. Zhang, L. Ouyang, and S. Yang, "The evaluation of solely renewable energy based virtual power plants potential for ancillary services provision," *IOP Conference Series: Earth and Environmental Science*, vol. 621, no. 1, 2021, doi: 10.1088/1755-1315/621/1/012064.

[19] B. Knopf, P. Nahmmacher, and E. Schmid, "The European renewable energy target for 2030 - An impact assessment of the electricity sector," *Energy Policy*, vol. 85, pp. 50–60, 2015, doi: 10.1016/j.enpol.2015.05.010.

[20] S. Impram, S. V. Nese, and B. Oral, "Challenges of renewable energy penetration on power system flexibility: A survey," *Energy Strategy Reviews*, vol. 31, p. 100539, Sep. 2020, doi: 10.1016/j.esr.2020.100539.

[21] S. Camal, F. Teng, A. Michiorri, G. Kariniotakis, and L. Badesa, "Scenario generation of aggregated Wind, Photovoltaics and small Hydro production for power systems applications," *Applied Energy*, vol. 242, pp. 1396–1406, May 2019, doi: 10.1016/j.apenergy.2019.03.112.

[22] N. Naval and J. M. Yusta, "Virtual power plant models and electricity markets - A review," *Renewable and Sustainable Energy Reviews*, vol. 149, p. 111393, Oct. 2021, doi: 10.1016/j.rser.2021.111393.

[23] C. Liu, R. J. Yang, X. Yu, C. Sun, P. S. P. Wong, and H. Zhao, "Virtual power plants for a sustainable urban future," *Sustainable Cities and Society*, vol. 65, p. 102640, Feb. 2021, doi: 10.1016/j.scs.2020.102640.

[24] M. Cai, S. Hu, Y. Wang, and J. Xiao, "A Dynamic Social Network Matching Model for Virtual Power Plants and Distributed Energy Resources with Probabilistic Linguistic Information," *Sustainability*, vol. 14, no. 22, p. 14920, Nov. 2022, doi: 10.3390/su142214920.

[25] S. Yu, F. Fang, Y. Liu, and J. Liu, "Uncertainties of virtual power plant: Problems and countermeasures," *Applied Energy*, vol. 239, pp. 454–470, Apr. 2019, doi: 10.1016/j.apenergy.2019.01.224.

[26] H. S. Moon, Y. G. Jin, Y. T. Yoon, and S. W. Kim, "Prequalification Scheme of a Distribution System Operator for Supporting Wholesale Market Participation of a Distributed Energy Resource Aggregator," *IEEE Access*, vol. 9, pp. 80434–80450, 2021, doi: 10.1109/ACCESS.2021.3085002.

[27] G. Yang, H. Liu, W. Wang, J. Chen, and S. Lei, "Distributed Optimal Coordination of a Virtual Power Plant with Residential Regenerative Electric Heating Systems," *Energies*, vol. 16, no. 11, p. 4314, May 2023, doi: 10.3390/en16114314.

[28] T. Chu, X. An, W. Zhang, Y. Lu, and J. Tian, "Multiple Virtual Power Plants Transaction Matching Strategy Based on Alliance Blockchain," *Sustainability*, vol. 15, no. 8, p. 6939, Apr. 2023, doi: 10.3390/su15086939.

[29] Y.-K. Wu, C.-L. Huang, Q.-T. Phan, and Y.-Y. Li, "Completed Review of Various Solar Power Forecasting Techniques Considering Different Viewpoints," *Energies*, vol. 15, no. 9, p. 3320, May 2022, doi: 10.3390/en15093320.

[30] A. W. Colman, R. J. Graham, and M. K. Davey, "Direct and indirect seasonal rainfall forecasts for East Africa using global dynamical models," *International Journal of Climatology*, vol. 40, no. 2, pp. 1132–1148, Feb. 2020, doi: 10.1002/joc.6260.

[31] N. Aoun, "Methodology for predicting the PV module temperature based on actual and estimated weather data," *Energy Conversion and Management: X*, vol. 14, 2022, doi: 10.1016/j.ecmx.2022.100182.

[32] J.-Y. Shin, K. R. Kim, and Y. H. Lee, "Spatial prediction of outdoor thermal comfort using an operational NWP model for city and regional scales: A case study in Korea," *Urban Climate*, vol. 45, p. 101286, Sep. 2022, doi: 10.1016/j.uclim.2022.101286.

[33] D. Cho, C. Yoo, B. Son, J. Im, D. Yoon, and D. H. Cha, "A novel ensemble learning for post-processing of NWP Model's next-day maximum air temperature forecast in summer using deep learning and statistical approaches," *Weather and Climate Extremes*, vol. 35, 2022, doi: 10.1016/j.wace.2022.100410.

[34] H. Zsiborács, G. Pintér, A. Vincze, N. H. Baranyai, and M. J. Mayer, "The reliability of photovoltaic power generation scheduling in seventeen European countries," *Energy Conversion and Management*, vol. 260, 2022, doi: 10.1016/j.enconman.2022.115641.

[35] Y. Liu and H. Liu, "Target Height Measurement under Complex Multipath Interferences without Exact Knowledge on the Propagation Environment," *Remote Sensing*, vol. 14, no. 13, p. 3099, Jun. 2022, doi: 10.3390/rs14133099.

[36] F. J. Diez, A. Martínez-Rodríguez, L. M. Navas-Gracia, L. Chico-Santamarta, A. Correa-Guimaraes, and R. Andara, "Estimation of the Hourly Global Solar Irradiation on the Tilted and Oriented Plane of Photovoltaic Solar Panels Applied to Greenhouse Production," *Agronomy*, vol. 11, no. 3, p. 495, Mar. 2021, doi: 10.3390/agronomy11030495.

[37] S. Barman, A. Chowdhury, S. Mathur, and J. Mathur, "Angular loss of window integrated thin film semi-transparent photovoltaic module," *Journal of Building Engineering*, vol. 40, 2021, doi: 10.1016/j.jobe.2021.102353.

[38] S. Barman, A. Chowdhury, S. Mathur, and J. Mathur, "Effectiveness of spectrally selective layer and airflow strategies in photovoltaic double pane window system," *Journal of Building Engineering*, vol. 62, p. 105417, Dec. 2022, doi: 10.1016/j.jobe.2022.105417.

[39] F. Shaik, S. S. Lingala, and P. Veeraboina, "Effect of various parameters on the performance of solar PV power plant: a review and the experimental study," *Sustainable Energy Research*, vol. 10, no. 1, 2023, doi: 10.1186/s40807-023-00076-x.

[40] K. Solbakken, Y. Birkelund, and E. M. Samuelsen, "Evaluation of surface wind using WRF in complex terrain: Atmospheric input data and grid spacing," *Environmental Modelling & Software*, vol. 145, p. 105182, Nov. 2021, doi: 10.1016/j.envsoft.2021.105182.

[41] M. El-Adll, H. M. Barakat, and A. Aly, "Asymptotic Prediction for Future Observations of a Random Sample of Unknown Continuous Distribution," *Complexity*, vol. 2022, pp. 1–15, Apr. 2022, doi: 10.1155/2022/4073799.

[42] G. Moreno, P. Martin, C. Santos, F. J. Rodriguez, and E. Santiso, "A Day-Ahead Irradiance Forecasting Strategy for the Integration of Photovoltaic Systems in Virtual Power Plants," *IEEE Access*, vol. 8, pp. 204226–204240, 2020, doi: 10.1109/ACCESS.2020.3036140.

[43] A. P. Foreman, C. C. St. Peter, G. A. Mesches, N. Robinson, and L. M. Romano, "Treatment Integrity Failures during Timeout from Play," *Behavior Modification*, vol. 45, no. 6, pp. 988–1010, Nov. 2021, doi: 10.1177/0145445520935392.

[44] L. Bauwens, P. Giot, J. Grammig, and D. Veredas, "A comparison of financial duration models via density forecasts," *International Journal of Forecasting*, vol. 20, no. 4, pp. 589–609, Oct. 2004, doi: 10.1016/j.ijforecast.2003.09.014.

[45] G. Narvaez *et al.*, "An interactive tool for visualization and prediction of solar radiation and photovoltaic generation in Colombia," *Big Earth Data*, vol. 7, no. 3, pp. 904–929, Jul. 2023, doi: 10.1080/20964471.2023.2185920.

[46] J. F. Barlow, "Excel Models for Business and Operations Management," 2005.

[47] S. Qin, B. X. Wang, W. Wu, and C. Ma, "The prediction intervals of remaining useful life based on constant stress accelerated life test data," *European Journal of Operational Research*, vol. 301, no. 2, pp. 747–755, Sep. 2022, doi: 10.1016/j.ejor.2021.11.026.

[48] A. Berger and M. Kiefer, "Comparison of Different Response Time Outlier Exclusion Methods: A Simulation Study," *Frontiers in Psychology*, vol. 12, Jun. 2021, doi: 10.3389/fpsyg.2021.675558.

[49] K. Nagashima, H. Noma, and T. A. Furukawa, "Prediction intervals for random-effects meta-analysis: A confidence distribution approach," *Statistical Methods in Medical Research*, vol. 28, no. 6, pp. 1689–1702, Jun. 2019, doi: 10.1177/0962280218773520.

[50] F. Wang, Z. Xuan, Z. Zhen, K. Li, T. Wang, and M. Shi, "A day-ahead PV power forecasting method based on LSTM-RNN model and time correlation modification under partial daily pattern prediction framework," *Energy Conversion and Management*, vol. 212, p. 112766, May 2020, doi: 10.1016/j.enconman.2020.112766.

[51] N. L. M. Jailani *et al.*, "Investigating the Power of LSTM-Based Models in Solar Energy Forecasting," *Processes*, vol. 11, no. 5, p. 1382, May 2023, doi: 10.3390/pr11051382.

[52] M. Husein and I.-Y. Chung, "Day-Ahead Solar Irradiance Forecasting for Microgrids Using a Long Short-Term Memory

Recurrent Neural Network: A Deep Learning Approach," *Energies*, vol. 12, no. 10, p. 1856, May 2019, doi: 10.3390/en12101856.
[53] T. Chai and R. R. Draxler, "Root mean square error (RMSE) or mean absolute error (MAE)? – Arguments against avoiding RMSE in the literature," *Geoscientific Model Development*, vol. 7, no. 3, pp. 1247–1250, Jun. 2014, doi: 10.5194/gmd-7-1247-2014.
[54] D. S. K. Karunasingha, "Root mean square error or mean absolute error? Use their ratio as well," *Information Sciences*, vol. 585, pp. 609–629, Mar. 2022, doi: 10.1016/j.ins.2021.11.036.
[55] M. Khandelwal, P. Mathuria, and R. Bhakar, "Virtual Power Plant (VPP) scheduling with uncertain multiple Locational Marginal Prices," *IET Energy Systems Integration*, vol. 4, no. 4, pp. 436–447, Dec. 2022, doi: 10.1049/esi2.12046.
[56] Y. Kim and Y. Byun, "Predicting Solar Power Generation from Direction and Tilt Using Machine Learning XGBoost Regression," *Journal of Physics: Conference Series*, vol. 2261, no. 1, p. 012003, Jun. 2022, doi: 10.1088/1742-6596/2261/1/012003.
[57] O. A. Al-Shahri *et al.*, "Solar photovoltaic energy optimization methods, challenges and issues: A comprehensive review," *Journal of Cleaner Production*, vol. 284, p. 125465, Feb. 2021, doi: 10.1016/j.jclepro.2020.125465.
[58] E. Kalkan, F. Y. Okur, and A. C. Altunışık, "Applications and usability of parametric modeling," *Journal of Construction Engineering, Management & Innovation*, vol. 1, no. 3, Oct. 2018, doi: 10.31462/jcemi.2018.03139146.

BIOGRAPHIES OF AUTHORS

Suwarno completed undergraduate electrical engineering education in 1986, completed postgraduate education in 1995 with the electrotechnical program, and completed the renewable energy doctoral program in 2016. Currently working at Universitas Muhammaddiyah Sumatera Utara in the Postgraduate Program and conducting research in the field of new and renewable energy, power electronics, and power electronics applications. He can be contacted at email: suwarno@umsu.ac.id.

Doni Pinayungan postgraduate student in the Electrical Engineering Masters Study Program, Universitas Muhammadiyah Sumatera Utara (UMSU), Medan, Indonesia. Received a Bachelor of Engineering degree in Electrical Engineering from the University of Riau Islands (UNRIKA) Batam in 2016. Currently, he is busy as an administrator for the North Padang Lawas Higher Education Foundation which oversees the North Padang Lawas Institute of Technology and Science (ITS PALUTA). Research interests include the fields of renewable energy, power electronics, and electronics applications. He can be contacted at email: donipinayungan@gmail.com.